482 *Inorg. Chem.* **2011**, *50*, 482–488
DOI: 10.1021/ic101413e

Inorganic Chemistry
Article

Metal-Binding Loop Length Is a Determinant of the pK_a of a Histidine Ligand at a Type 1 Copper Site

Chan Li,[†] Katsuko Sato,[†] Stefano Monari,[‡] Isabelle Salard,[†] Marco Sola,[‡] Mark J. Banfield,[§] and Christopher Dennison*,[†]

[†]*Institute for Cell and Molecular Biosciences, Medical School, Newcastle University, Newcastle upon Tyne NE2 4HH, U.K.,* [‡]*Department of Chemistry, University of Modena and Reggio Emilia, Via Campi 183, 41125 Modena, Italy, and* [§]*Department of Biological Chemistry, John Innes Centre, Norwich NR4 7UH, U.K.*

Received July 15, 2010

The type 1 copper site of a cupredoxin involves coordination by cysteine, histidine, and methionine residues from a single loop. Dissociation and protonation of the histidine ligand on this loop is observed in only certain reduced cupredoxins and can regulate electron-transfer reactivity. This effect is introduced in azurin (AZ) (the wild-type protein has an estimated pK_a of <2) by mutating the native copper-binding loop (C^{112}TFPGH^{117}SALM^{121}, ligands numbered). In this work, we have investigated the influence of loop length alone on histidine ligand protonation by determining the pK_a value in AZ variants with ligand-containing polyalanine loops of different length. Crystal structures of the Cu(I)-variant with the loop sequence C^{112}AAH^{115}AAM^{118} (AZ2A2A) demonstrate that at pH 4.2 His115 is protonated and no longer coordinated, and the imidazole ring is rotated by 180°. The influence of pH on the reduction potential allows a pK_a of 5.2 ± 0.1 for His115 in Cu(I)-AZ2A2A to be determined. In the reduced AZ variants in which the loop sequences C^{112}AAAAH^{117}AAAM^{121} (AZ4A3A) and C^{112}AAAAH^{117}AAAAM^{122} (AZ4A4A) have been introduced, pK_a values of 4.5 ± 0.1 and 4.4 ± 0.1, respectively, are obtained for the His117 ligand. Consistent with these data, the crystal structure of Cu(I)-AZ4A4A at pH 5.3 shows no sign of His117 protonation (crystals were unstable at lower pH values). The loop length range studied matches that which occurs naturally and these investigations indicate that length alone can alter the pK_a of the coordinating histidine by approximately 1 pH unit. The pK_a for this histidine ligand varies in native cupredoxins by >5 pH units. Other structural and electronic features, governed primarily by the second-coordination sphere, to which the ligand-binding loop is a major contributor, also alter this important feature. A longer ligand-containing loop made of residues whose side chains are larger and more complex than a methyl group increases the second coordination sphere providing additional scope for tuning the pK_a of the histidine ligand and other active site properties.

Introduction

Metals are essential for the function of many proteins, and copper and iron are routinely used for electron transfer (ET). The protonation of the amino acids that coordinate metals can have functional importance, and deciphering the factors that control the pK_a values of ligating residues is therefore crucial. This is particularly the case for ET metalloproteins because electron and proton transfer is coupled in biological systems. When nature utilizes copper for ET, it is nearly always encased in a rigid β-barrel scaffold (cupredoxin fold) resulting in a constrained geometry for the metal.[1−3] The resulting copper site is classified as type 1 (T1) and undergoes minimal change upon redox interconversion, giving rise to a small reorganization energy and fast ET. The majority of the ligands at a T1 copper site; a cysteine, histidine, and methionine, are provided by a single C-terminal loop (Figure 1).[1,3] The only identified ET switch in T1 copper-containing proteins involves the histidine ligand on this loop, which has been found to dissociate from Cu(I) and protonate in certain cupredoxins.[3−7] The resulting positively charged imidazolium and three-coordinate Cu(I) center have a dramatic effect on the reduction potential (E_m) and ET reactivity[3,8−10] and

*To whom correspondence should be addressed. E-mail: christopher.dennison@ncl.ac.uk.

(1) Adman, E. T. *Adv. Protein Chem.* **1991**, *42*, 145–197.
(2) Gray, H. B.; Malmström, B. G.; Williams, R. J. P. *J. Biol. Inorg. Chem.* **2000**, *5*, 551–559.
(3) Dennison, C. *Coord. Chem. Rev.* **2005**, *249*, 3025–3054.
(4) Guss, J. M.; Harrowell, P. R.; Murata, M.; Norris, V. A.; Freeman, H. C. *J. Mol. Biol.* **1986**, *192*, 361–387.
(5) Dennison, C.; Kohzuma, T.; McFarlane, W.; Suzuki, S.; Sykes, A. G. *Chem. Commun.* **1994**, 581–582.
(6) Vakoufari, E.; Wilson, K. S.; Petratos, K. *FEBS Lett.* **1994**, *347*, 203–206.
(7) Zhu, Z.; Cunane, L. M.; Chen, Z. W.; Durley, R. C. E.; Mathews, F. S.; Davidson, V. L. *Biochemistry* **1998**, *37*, 17128–17136.
(8) Di Bilio, A. J.; Dennison, C.; Gray, H. B.; Ramirez, B. E.; Sykes, A. G.; Winkler, J. R. *J. Am. Chem. Soc.* **1998**, *120*, 7551–7556.

 Published on Web 12/08/2010 © 2010 American Chemical Society

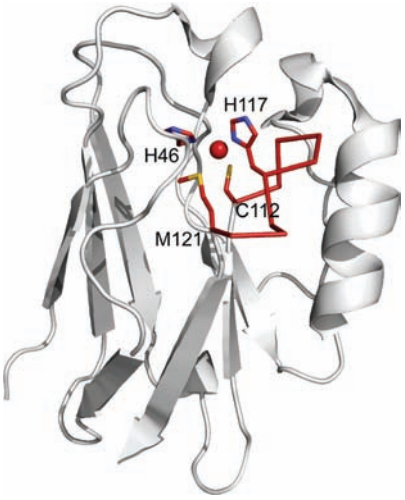

Figure 1. The structure of AZ with the C-terminal ligand-containing loop shown as a C^{α} trace, the coordinating residues as stick models and the copper ion as a sphere (all dark red).

provides a mechanism whereby protons can regulate a cupredoxin-containing ET pathway.[4,7]

Protonation of the C-terminal histidine ligand is only accessible in certain cupredoxins and is not normally observed in azurin (AZ), where a pK_a of < 2 has been estimated for the wild-type (WT) protein.[11] Replacement of the native loop (C^{112}TFPGH^{117}SALM^{121}; ligands numbered) with the shorter loops from cupredoxins that exhibit this effect, such as amicyanin (AMI) and plastocyanin (PC), gives rise to chimeras in which the histidine ligand protonates.[12,13] Similar mutations in AMI, PC, and pseudoazurin (PAZ) also affect the pK_a of the histidine.[12−16] The ligand-containing loop seems to be important for histidine ligand protonation, but sequence variations in the chimeras studied to date make it impossible to discern the influence of length alone.

Other aspects of the active sites of cupredoxins have been suggested to influence the pK_a of the histidine ligand including hydrogen bonding and π-interactions.[3,5,9,11−13,16−27] The majority of these arise from the second-coordination sphere of the copper and have also been shown to affect the E_m value and ET reactivity.[21,23,24,26,28,29] The ligand-containing loop makes a significant contribution to the second coordination sphere of a T1 copper site, and these two features are therefore closely linked. A series of AZ mutants has recently been constructed in which non-native polyalanine loops of differing length have been introduced in place of the native sequence.[30] The methyl groups on these loops are sufficiently bulky to protect the copper site from solvent but make a limited contribution to the second-coordination sphere. The structures of these variants demonstrate that loop length and not sequence dictates the structure of this region.[30] In our previous studies, we did not investigate the influence of pH on the active site properties of any of these variants. Herein we describe the influence of pH on the Cu(I) site of AZ2A2A (two alanine residues between the cysteine and histidine and histidine and methionine ligands; the shortest loop length as found in AMI), AZ4A3A (whose loop length matches that of AZ), and AZ4A4A (longest loop length that naturally occurs in cupredoxins). We find that the pK_a of the histidine ligand depends on the length of the loop, making it one of a number of features that can tune this important ET switch.

Experimental Section

Proteins. The *Pseudomonas aeruginosa* azurin (AZ) variants in which the Cys112 to Met121 loop (C^{112}TFPGH^{117}SALM^{121}) has been replaced with the C^{112}AAH^{115}AAM^{118} (AZ2A2A), C^{112}AAAAH^{117}AAAM^{121} (AZ4A3A), and C^{112}AAAAH^{117}-AAAAM^{122} (AZ4A4A) sequences were isolated and purified as described previously.[30]

Crystallization, Data Collection, and Structure Determination. Cu(II)-AZ2A2A was crystallized as described previously.[30] Crystals of Cu(II)-AZ2A2A were reduced by transferring them into 20 μL of reservoir buffer containing 10 mM ascorbate (pH 7.0). Reduction was considered to be complete when the crystal was totally colorless (typically $\sim$1 h). A reduced crystal was transferred to well solution [0.2 M potassium thiocyanate, 30% poly(ethylene glycol) (PEG) 2000] plus 10 mM ascorbate, the pH of which had been adjusted to 4.8. The crystal was left in this lower pH solution for $>$1.5 h prior to being immersed in a cryo-buffer comprised of 10% glycerol, 0.1 M potassium thiocyanate, 32% PEG 2000, and 10 mM ascorbate at pH 4.8. A similar experiment was performed at pH 4.2, but in this case, the reduced crystal was soaked in the low pH solution for 40 min and immersed in *N*-paratone oil as a cryoprotectant. Cu(II)-AZ4A4A was crystallized as described previously,[30] and crystals

(9) Battistuzzi, G.; Borsari, M.; Canters, G. W.; de Waal, E.; Leonardi, A.; Ranieri, A.; Sola, M. *Biochemistry* **2002**, *41*, 14293–14298.
(10) Sato, K.; Kohzuma, T.; Dennison, C. *J. Am. Chem. Soc.* **2003**, *125*, 2101–2112.
(11) Jeuken, L. J. C.; van Vliet, P.; Verbeet, M. P.; Camba, R.; McEvoy, J. P.; Armstrong, F. A.; Canters, G. W. *J. Am. Chem. Soc.* **2000**, *122*, 12186–12194.
(12) Yanagisawa, S.; Dennison, C. *J. Am. Chem. Soc.* **2004**, *126*, 15711–15719.
(13) Li, C.; Banfield, M. J.; Dennison, C. *J. Am. Chem. Soc.* **2007**, *129*, 709–718.
(14) Dennison, C.; Vijgenboom, E.; Hagen, W. R.; Canters, G. W. *J. Am. Chem. Soc.* **1996**, *118*, 7406–7407.
(15) Buning, C.; Canters, G. W.; Comba, P.; Dennison, C.; Jeuken, L.; Melter, M.; Sanders-Loehr, J. *J. Am. Chem. Soc.* **2000**, *122*, 204–211.
(16) Battistuzzi, G.; Borsari, M.; Canters, G. W.; Di Rocco, G.; de Waal, E.; Arendsen, Y.; Leonardi, A.; Ranieri, A.; Sola, M. *Biochemistry* **2005**, *44*, 9944–9949.
(17) Guss, J. M.; Merritt, E. A.; Phizackerley, R. P.; Freeman, H. C. *J. Mol. Biol.* **1996**, *262*, 686–705.
(18) Kohzuma, T.; Inoue, T.; Yoshizaki, F.; Sasakawa, Y.; Onodera, K.; Nagatomo, S.; Kitagawa, T.; Uzawa, S.; Isobe, Y.; Sugimura, Y.; Gotowda, M.; Kai, Y. *J. Biol. Chem.* **1999**, *274*, 11817–11823.
(19) Bond, C. S.; Blankenship, R. E.; Freeman, H. C.; Guss, J. M.; Maher, M. J.; Selvaraj, F. M.; Wilce, M. C. J.; Willingham, K. M. *J. Mol. Biol.* **2001**, *306*, 47–67.
(20) Dennison, C.; Lawler, A. T.; Kohzuma, T. *Biochemistry* **2002**, *41*, 552–560.
(21) Machczynski, M. C.; Gray, H. B.; Richards, J. H. *J. Inorg. Biochem.* **2002**, *88*, 375–380.
(22) Rooney, M. B.; Honeychurch, M. J.; Selvaraj, F. M.; Blankenship, R. E.; Bond, A. M.; Freeman, H. C. *J. Biol. Inorg. Chem.* **2003**, *8*, 306–317.
(23) Carrell, C. J.; Sun., D.; Jiang, S.; Davidson, V. L.; Mathews, F. S. *Biochemistry* **2004**, *43*, 9372–9380.
(24) Yanagisawa, S.; Banfield, M. J.; Dennison, C. *Biochemistry* **2006**, *45*, 8812–8822.
(25) Li, C.; Yanagisawa, S.; Martins, B. M.; Messerschmidt, A.; Banfield, M. J.; Dennison, C. *Proc. Natl. Acad. Sci. U.S.A.* **2006**, *103*, 7258–7263.
(26) Yanagisawa, S.; Crowley, P. B.; Firbank, S. J.; Lawler, A. T.; Hunter, D. M.; McFarlane, W.; Li, C.; Kohzuma, T.; Banfield, M. J.; Dennison, C. *J. Am. Chem. Soc.* **2008**, *130*, 15420–15428.
(27) Su, P.; Li, H. *Inorg. Chem.* **2010**, *49*, 435–444.
(28) Lancaster, K. M.; DeBeer George, S.; Yokoyama, K.; Richards, J. H.; Gray, H. B. *Nat. Chem.* **2009**, *1*, 711–715.
(29) Marshall, N. M.; Garner, D. K.; Wilson, T. D.; Gao, Y. G.; Nilges, M. J.; Lu, Y. *Nature* **2009**, *462*, 113–116.
(30) Sato, K.; Li, C.; Salard, I.; Thompson, A. J.; Banfield, M. J.; Dennison, C. *Proc. Natl. Acad. Sci. U.S.A.* **2009**, *106*, 5616–5621.

Table 1. Crystallographic Data Collection and Refinement Statistics

	Cu(I)-AZ2A2A, pH 4.8	Cu(I)-AZ2A2A, pH 4.2	Cu(I)-AZ4A4A, pH 5.3
		Data Collection	
space group	$P2_12_12_1$	$P2_12_12_1$	$P2_1$
resolution (Å)[a,b]	40.0−1.60 (1.69−1.60)	57.74−1.60 (1.68−1.60)	29.49−2.30 (2.42−2.30)
unit cell (Å, deg)[b,c]	a = 39.99, b = 46.15, c = 57.93	a = 39.90, b = 46.25, c = 57.84	a = 34.43, b = 86.59, c = 41.70, β = 114.43
no. unique reflns[b,c]	14711 (2082)	14745 (2045)	9493 (1294)
redundancy[b,c]	10.1 (9.8)	6.7 (5.9)	6.4 (6.4)
$I/\sigma(I)$[a,b,c]	45.6 (14.1)	25.6 (7.0)	18.9 (5.0)
completeness (%)	100.0 (99.8)	99.7 (97.7)	95.9 (92.1)
R_{merge} (%)[b,c]	3.4 (14.8)	5.8 (21.3)	9.6 (34.6)
		Refinement	
resolution (Å)[b]	40.0−1.60 (1.64−1.60)	36.13−1.60 (1.64−1.60)	29.49−2.30 (2.36−2.30)
R_{factor} (%)[b,d]	14.7 (18.0)	14.0 (15.2)	18.3 (23.7)
R_{free} (%)[b,d]	19.9 (27.0)	20.0 (28.1)	26.6 (33.0)
rmsd bond lengths (Å)	0.017	0.017	0.013
rmsd bond angles (deg)	1.58	1.68	1.47
no. non-hydrogen atoms	1117	1149	2041
avg *B*-factor (protein, Å^2)	14.2	14.2	19.4
avg *B*-factor (ligands, Å^2)	24.0	25.3	18.1
ESU (maximum likelihood, Å)	0.050	0.054	0.221
Ramachandran favored (%)[e]	97.6	97.5	96.1
Ramachandran outliers (%)[e]	0.0	0.0	0.0

[a] The high resolution limit was restricted to 1.6 Å by the constraints of the data collection setup. [b] Values in parentheses are those for the highest resolution shell. [c] Reflection statistics are as reported by SCALA. R_{merge} is calculated as described in ref 36. [d] $R_{free} = \sum(|F_{obs}| - |F_{calc}|)/\sum|F_{obs}|$, where $|F_{obs}|$ are observed structure factor amplitudes for a given reflection and $|F_{calc}|$ are corresponding calculated structure factor amplitudes obtained from the refined model. R_{free} uses only those reflections set aside as a "test set". R_{cryst} is calculated as per R_{free} but using the "working set" of reflections. [e] As calculated by MOLPROBITY.[38]

were reduced by transferring them into 15 μL of the reservoir buffer containing 10 mM ascorbate (pH 7.0) typically for ~1 h. A reduced crystal was transferred to well solution (10 mM trisodium citrate, 33% PEG 6000) plus 10 mM ascorbate whose pH had been adjusted to 5.3. The crystal was left in this lower pH solution for >1 h prior to being directly frozen. Reduced AZ4A4A crystals were also transferred to well solution that had been adjusted to pH 4.5. Diffraction from these crystals was very poor and useable data could not be obtained.

Protein crystals were maintained at cryogenic temperatures during data collection. Diffraction data were collected on a home source using X-rays from a Rigaku Micromax-007 generator with Osmic optics and a Rigaku Raxis IV^{++} image plate detector. All data were processed with iMOSFLM[31] and scaled with SCALA.[32] Data collection and processing statistics are given in Table 1. Structures were solved either by direct refinement (AZ2A2A structures) or molecular replacement (AZ4A3A structure). For the Cu(I) AZ2A2A structures at pH 4.8 and 4.2, the model of the oxidized protein [PDB code 3FS9[30]] was directly refined with the new data following removal of all water molecules. The structure of Cu(I) AZ4A4A at pH 5.3 was solved using MOLREP (as implemented in CCP4[33]) with a monomer of the oxidized structure [PDB code 3FSZ[30]] as the search model (waters removed). Iterative model building [using COOT[34]] and refinement cycles [REFMAC5, as implemented in CCP4] were used to complete the structures.[35,36] Final refinement statistics are given in Table 1. Structures were superimposed and rmsds for C^α atoms were calculated using LSQMAN.[37] Ramachandran plots were generated in MOLPROBITY,[38] and protein figures were prepared using PYMOL (see http://pymol.org). The coordinates and structure factors have been submitted to the Protein Data Bank (PDB) with codes 2xv0 [Cu(I)-AZ2A2A at pH 4.8], 2xv2 [Cu(I)-AZ2A2A at pH 4.2], and 2xv3 [Cu(I)-AZ4A4A at pH 5.3].

Electrochemistry of Proteins. Cyclic voltammetry (CV) experiments (22 ± 1 °C) were performed using electrochemical setups described previously.[9,20] All midpoint potentials (E_m values) are referenced to the normal hydrogen electrode (NHE), and voltammograms were calibrated either using the $[Co(phen)_3]^{3+/2+}$ or the MV^{2+}/MV^+ (MV = methyl viologen) couple. Gold working electrodes were modified using a saturated solution of 4,4-dithiodipyridine (Aldrithiol-4) for AZ2A2A and a 1 mM solution of 4-mercaptopyridine for AZ4A3A and AZ4A4A. For experiments with AZ2A2A, the pH was altered using a pH jump method described previously (I = 0.10 M, NaCl).[12] AZ4A3A and AZ4A4A were in 20 mM tris(hydroxymethyl)aminomethane (Tris), and the pH was adjusted by adding small amounts of NaOH or HCl under fast stirring. Final protein concentrations were typically 100−200 μM. For all CVs, the anodic and cathodic peaks had very similar intensities proportional to (scan rate)$^{1/2}$ indicating that ET is diffusion controlled. The pH dependence of E_m for AZ2A2A, AZ4A3A, and AZ4A4A in the pH ranges 5.5−4.2, 5.2−3.5, and 4.7−3.4, respectively, were fit to eq 1:

$$E_m(\text{pH}) = E_m(\text{high pH}) + RT/(nF)\ln(1 + [H^+]/K_a^{red}) \quad (1)$$

where E_m(pH) is the measured E_m at a particular pH value, E_m(high pH) is the E_m at high pH, K_a^{red} is the proton dissociation constant for the residue in the reduced protein, which affects

(31) Leslie, A. G. *Acta Crystallogr. D: Biol. Crystallogr.* **2006**, *62*, 48–57.
(32) Evans, P. *Acta Crystallogr. DL Biol. Crystallogr.* **2006**, *62*, 72–82.
(33) Vagin, A.; Teplyakov, A. *J. Appl. Crystallogr.* **1997**, *30*, 1022–1025.
(34) Emsley, P.; Cowtan, K. *Acta Crystallogr. D: Biol. Crystallogr.* **2004**, *60*, 2126–2132.
(35) Murshudov, G. N.; Vagin, A. A.; Dodson, E. J. *Acta Crystallogr. D: Biol. Crystallogr.* **1997**, *53*, 240–255.
(36) Collaborative computational project *Acta Crystallogr. D: Biol. Crystallogr.* **1994**, *50*, 760–763.
(37) Kleywegt, G. J.; Zou, J. Y.; Kjeldgaard, M., Jones, T. A. In *Crystallography of biological macromolecules* Rossmann, M. G.; Arnold, E., Eds.; International tables for crystallography, Vol. *F*; Kluwer: Dordrecht, The Netherlands, 2001; pp 353−356 and 366−367.
(38) Chen, V. B.; Arendall, W. B., 3rd; Headd, J. J.; Keedy, D. A.; Immormino, R. M.; Kapral, G. J.; Murray, L. W.; Richardson, J. S.; Richardson, D. C. *Acta Crystallogr. D: Biol. Crystallogr.* **2010**, *66*, 12–21.
(39) Nar, H.; Messerschmidt, A.; Huber, R.; Van de Kamp, M.; Canters, G. W. *J. Mol. Biol.* **1991**, *221*, 765–772.

E_m(pH) as the pH value is lowered. The errors quoted for K_a^{red} values are those obtained from the fits of the data (the actual experimental error could be slightly larger).

Results

As the pH is lowered, the overall structure of Cu(I)-AZ2A2A is unaffected (rmsds of 0.10 and 0.14 Å for the structures at pH 4.8 and 4.2, respectively, compared with that at pH 7.0), but alterations at the Cu(I) site are observed (Figure 2 and Table 2). At pH 4.8, the Cu(I)−N^{δ}(His115) bond lengthens by 0.25 Å (Table 2). The estimated standard uncertainties (ESUs), as reported by REFMAC5, for the AZ2A2A structures at pH 7.0[30] and 4.8 (Table 1) are 0.010 and 0.050, respectively (Cu−ligand distances would be expected to exhibit higher precision[28]), and the change observed is therefore significant. This increase is indicative of the onset of His115 protonation with the average of two forms observed in the electron density, as described previously in crystallographic studies on poplar PC.[4] At pH 4.2, His115 has moved much further from the copper ion, consistent with the protonated form being the major species present. In this structure, the histidine can be modeled in two distinct conformations, one in which the imidazole has not rotated compared with the coordinated arrangement and another in which the ring has rotated by 180°. Although it is difficult to discern between these based on the electron density, the hydrogen bonding pattern suggests that the rotated conformation (Figure 2 and Table 2) is the dominant species. In particular, in this conformation the imidazole forms a hydrogen bond via its $N^{\varepsilon 2}H$ atom with the backbone carbonyl oxygen of Gly45, an interaction that is also found between the corresponding residues in Cu(I) poplar PC at low pH.[4] The Cu(I) to O(Gly45) distance is unaltered at pH 4.2, but the metal moves closer to Met118 (2.8 Å from the metal) providing a weak interaction and resulting in a three-coordinate Cu(I) site with a highly distorted trigonal planar geometry (Table 2).

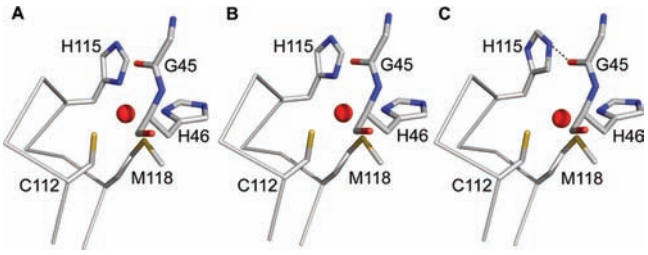

Figure 2. The structures of the Cu(I) site and the ligand-containing loop of AZ2A2A at pH 7.0 (A), 4.8 (B), and 4.2 (C). The hydrogen bond formed between the $N^{\varepsilon 2}$ of His115 and the backbone carbonyl of Gly45 in the structure at pH 4.2 in which the imidazole ring is rotated is shown as a dashed line. The N−H···O distance and angle are 2.62 Å and 120°, respectively.

The overall structure (rmsd for C^{α} atoms of 0.29 Å) and the conformation of the mutated loop in Cu(I)-AZ4A4A are similar at pH 7.0 and 5.3. Repeated attempts to obtain a structure of this reduced variant at lower pH were unsuccessful due to poor diffraction, probably as a consequence of crystal damage upon acidification. There is no sign of His117 dissociation and protonation at pH 5.3 (Table 2). There are small increases in the Cu(I)−N^{δ}(His117) bond length and the Cu(I) to S^{δ}(Met122) interaction (Table 2), which, considering the ESU of 0.221 Å (Table 1) for the AZ4A4A structure at pH 5.3 [the ESU is 0.11 for the Cu(I) structure at approximately neutral pH[30]], are probably not significant.

To demonstrate histidine ligand protonation in solution and to determine the pK_a of this residue, the influence of pH on E_m has been measured (Figure 3A). In AZ, the changes in E_m in the pH 5.5−8.0 range (Figure 3A) are due to the protonation/deprotonation of the noncoordinating His35 and His83 residues,[40−42] with the former having the largest influence [pK_a^{ox} (for the oxidized protein) and pK_a^{red} values of 6.5 and 7.3, respectively, have been determined for His35 and 7.5 and 7.7 for His83 in WT AZ[40]]. Below pH 5.5, the E_m value of the WT protein is almost unaffected by pH (a small decrease is found below pH 3.5).[41,42] In AZ2A2A, a similar effect as observed in the WT protein also occurs above pH 5.5, although the influence on E_m is smaller. The E_m value of AZ2A2A increases with decreasing pH in the 5.5−4.2 range (the electrochemical response deteriorates dramatically at pH values below 4.2) with a limiting slope of approximately

Table 2. The Cu(I) Site Geometries in AZ at pH 5.5, AZ2A2A at pH 7,[30] 4.8, and 4.2, and AZ4A4A at pH 7[30] and 5.3[a]

	AZ, pH 5.5[b]	AZ2A2A, pH 7	AZ2A2A, pH 4.8	AZ2A2A, pH 4.2	AZ4A4A, pH 7[c]	AZ4A4A, pH 5.3[c]
			Cu(I)−Ligand Bond Distances (Å)			
Cu−O(Gly45)	3.02	3.49	3.51	3.61	3.36	3.27
Cu−$N^{\delta 1}$(His46)	2.14	2.03	2.14	2.02	2.12	2.02
Cu−S^{γ}(Cys112)	2.29	2.21	2.16	2.13	2.19	2.15
Cu−$N^{\delta 1}$(His115/117)	2.10	2.02	2.27		2.10	2.23
Cu−S^{δ}(Met118/122)	3.25	3.04	3.00	2.81	3.23	3.29
			Angle (deg)			
Gly45−Cu−His46	75	71	71	69	75	80
Gly45−Cu−Cys112	99	98	97	95	99	102
Gly45−Cu−His115/117	87	79	72		81	81
Gly45−Cu−Met118/122	145	148	146	144	144	145
His46−Cu−Cys112	133	131	133	143	138	136
His46−Cu−His115/117	105	102	102		99	104
His46−Cu−Met118/122	73	81	80	85	75	70
Cys112−Cu−His115/117	122	122	118		123	120
Cys112−Cu−Met118/122	114	112	116	121	117	113
His115/117−Cu−Met118/122	88	93	97		84	90

[a] The residue numbering is as found in AZ2A2A/AZ4A4A. In AZ His117 and Met121 are ligands. [b] Average of the four molecules in the asymmetric unit.[39] [c] Average of the two molecules in the asymmetric unit.

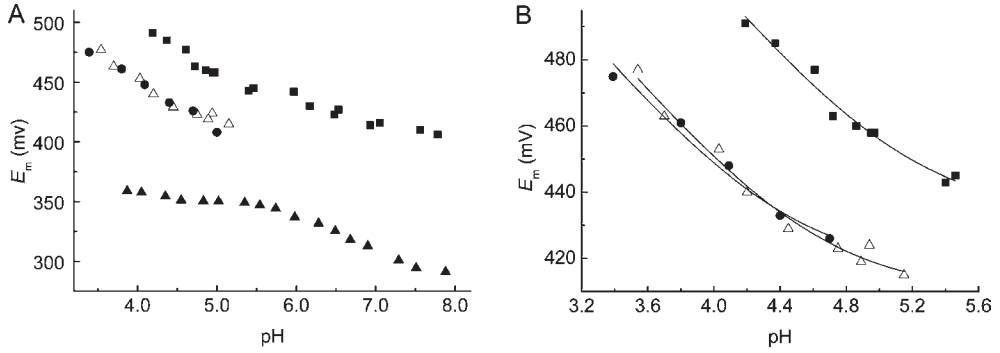

Figure 3. The pH dependence of E_m for AZ (▲),[12] AZ2A2A (■), AZ4A3A (Δ), and AZ4A4A (●) is shown in panel A. In panel B, the data for AZ2A2A (■), AZ4A3A (Δ), and AZ4A4A (●) at low pH are fit to eq 1 giving pK_a^{red} values of 5.2 ± 0.1, 4.5 ± 0.1, and 4.4 ± 0.1, respectively. Inclusion of the point at pH 5.0 for AZ4A4A increases pK_a^{red} slightly but decreases the quality of the fit.

−60 mV/pH. This can be assigned to the protonation of His115 upon reduction, and a pK_a^{red} of 5.2 ± 0.1 is obtained from a fit of the data to eq 1 (Figure 3B). For AZ4A3A and AZ4A4A, limited data have been acquired above pH 5, and the alterations in E_m in this region are larger than those for the WT protein (data not shown). We are currently unsure about the cause of the differences observed in this pH range for the different loop mutants. However, a comparison of the crystal structures of AZ4A4A at pH 7 and pH 5.3 (and those of AZ2A2A at pH 7.0, 4.8, and 4.2) show no major structural changes in the region of His35 or His83 compared with the WT protein. The data below pH 5.2 and 4.8 for AZ4A3A and AZ4A4A, respectively, also show an increase in E_m and fits to eq 1 (Figure 3B) give pK_a^{red} values of 4.5 ± 0.1 and 4.4 ± 0.1, respectively.

Discussion

The Effect of Loop Length on the Histidine Ligand pK_a. In this study, we demonstrate, using AZ as a model system, that the naturally occurring loop length range at a T1 copper site can influence the pK_a of the coordinating histidine on the loop by approximately 1 pH unit. The alterations in loop length could have influenced the flexibility of this region which may affect the pK_a. However, the *B*-factors are low (typically < 20) for loop residues in all of the variants and compare favorably with those for amino acids in the core of each individual protein (as is also the case in the WT protein). Molecular dynamics simulations could provide insight about changes in mobility in this region upon making these loop mutations, although recent studies on other AZ loop-contraction variants do not highlight any dramatic effects.[43] Further studies are required to determine the relationship between loop length and the dynamics of this region. The pK_a of His115 is almost the same in Cu(I)-AZ2A2A (5.2 ± 0.1) and Cu(I)-AZAMI (5.5 ± 0.1),[12] which possess the same loop length but with very different sequences (CAAHAAM versus CTPHPFM). The loop and active site structures are remarkably similar in AZ2A2A and AZAMI, with the loops having almost identical conformations as that in AMI.[25,30] In AMI from different organisms, the pK_a values are higher and vary from 6.5 to 7.7.[7,9,14] Lipocyanin, a cupredoxin whose structure has not been determined, possesses the same loop length as AMI but with a slightly different sequence (CTIHPFM), yet the histidine pK_a is ≪4.[44] The pK_a for His117 in Cu(I)-AZ4A3A is considerably higher than that estimated for WT AZ (< 2),[11] even though they possess the same loop length and structure.[30] This is also the case for Cu(I)-AZ4A4A, whose histidine ligand pK_a value is much higher than those for auracyanin B and rusticyanin (RST), which have the same loop length and structure[30] and do not exhibit histidine ligand protonation in the accessible pH range.[16,22] The histidine ligand pK_a exhibits a much greater range in cupredoxins (> 5 pH units) than that observed in the polyalanine AZ loop mutants, demonstrating that loop length is only one of a number of features that can influence this feature. The C-terminal loops of cupredoxins make a significant contribution to the second coordination sphere at a T1 copper site. The number of interactions from this region is diminished by a shorter loop and also by the presence of only alanine side chains in the loop (*vide infra*).

The Role of Active Site Hydrogen Bonding on the Histidine Ligand pK_a. The hydrogen bonding pattern around T1 copper sites is a second coordination sphere feature that has been implicated in influencing the pK_a of the histidine ligand. However, the overall hydrogen-bonding pattern is very similar at the active sites of AZ2A2A (Figure 4), AZAMI, AMI, AZ4A3A, and AZ. Two additional hydrogen bonds, resulting from the extra residue adjacent to the methionine ligand, are found in AZ4A4A, auracyanin B, and RST, but these cannot be responsible for the very low pK_a values of the histidine ligand in only the latter two proteins. The hydrogen bonds to the coordinating thiolate sulfur of the cysteine ligand have been suggested to be particularly important for the pK_a of the histidine ligand. The native cupredoxins in which histidine ligand protonation is not observed have two hydrogen bonds to this ligating atom.[17,19−21] These are provided by the backbone amides of the residue adjacent to the N-terminal histidine ligand, which is usually an

(40) Van de Kamp, M.; Canters, G. W.; Andrew, C. R.; Sanders-Loehr, J.; Bender, C. J.; Peisach, J. *Eur. J. Biochem.* **1993**, *218*, 229–238.
(41) Strong St. Clair, C.; Ellis, W. R.; Gray, H. B. *Inorg. Chim. Acta* **1992**, *191*, 149–155.
(42) Jeuken, L. J. C.; Wisson, L. J.; Armstrong, F. A. *Inorg. Chim. Acta* **2002**, *331*, 216–223.
(43) Rajapandian, V.; Hakkim, V.; Subramanian, V. *J. Phys. Chem. B* **2010**, *114*, 8474–8486.
(44) Worrall, J. A. R.; Machczynski, M. C.; Keijser, B. J. F.; Di Rocco, G.; Ceola, S.; Ubbink, M.; Vijgenboom, E.; Canters, G. W. *J. Am. Chem. Soc.* **2006**, *128*, 14579–14589.

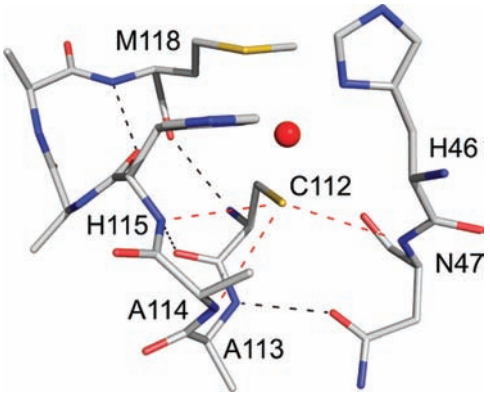

Figure 4. The hydrogen-bonding pattern around the Cu(I) site of AZ2A2A. The hydrogen bonds to the cysteine ligand are shown as dashed red lines, while all other hydrogen bonds are black. The N−H···S$^{\gamma}$ hydrogen-bonding distances are 2.68, 2.78, and 2.72 Å for the backbone amides of Asn47, Ala114, and His115, respectively, while the hydrogen-bonding angles are 166°, 129°, and 147°.

asparagine (Asn47 in AZ), and the backbone amide of the residue two after the coordinating cysteine (Phe114 in AZ).[19,39,45] The N−H···S$^{\gamma}$ hydrogen bonding distance and angle are typically ∼2.6 Å (N to S distance of ∼3.5 Å) and ∼160°, respectively, with the latter suggested to be optimal for this interaction.[23] The removal of one of these hydrogen bonds in the Phe114Pro AZ variant does not result in His117 protonation being observed above pH 4.[24] In AMI, AZAMI, PC, AZPC, PAZ, and PAZAMI a proline is found in the corresponding position, and this interaction is therefore absent in these proteins.[13,25,46−49] In AMI, the mutation of this proline (Pro94) to alanine and phenylalanine results in the introduction of the second hydrogen bond[23] and a decrease in the pK_a of His95,[21] with a much larger effect in the Pro94Phe variant. The N−H···S$^{\gamma}$ hydrogen-bonding angles in these AMI mutants (∼130°) seem to be less than optimal,[23] and the effect of the mutations on the pK_a was suggested to be due to steric factors.[23] In AZ2A2A there are probably three hydrogen bonds to the coordinating thiolate, provided by the backbone amides of Asn47, Ala114, and also His115 (Figure 4). The N−H···S$^{\gamma}$ hydrogen-bonding angles would indicate that the interactions involving Asn47 and His115 are stronger. In AZAMI, the backbone amide of His115 also seems to form a second hydrogen bond with the coordinating thiolate (N to S distance of 3.7 Å). A similar, albeit longer (≥3.9 Å), interaction is present in AMI, PC, PAZ, AZAMI-F, and PAZAMI,[13,25,46−49] and its influence is therefore probably less significant. Hydrogen bonding to the cysteine ligand has a limited influence on the pK_a of the coordinating histidine.

Hydrogen bonds involving the C-terminal histidine ligand are potentially more influential as far as the pK_a of this residue is concerned. In Cu(I)-AZ2A2A, a hydrogen bond forms between the N$^{\varepsilon 2}$ of the protonated and rotated conformation of His115 and the backbone carbonyl of Gly45 (Figure 2C). The N−H···O distance and angle are 2.62 Å (3.14 Å between N and O atoms) and 120°, respectively, compared with values of 2.42 Å and 137° for the corresponding hydrogen bond between the N$^{\varepsilon 2}$H atom of His87 and the backbone carbonyl oxygen of Pro36 in the low-pH structure of Cu(I) poplar PC.[4] A similar interaction is found in the protonated and rotated conformer of His115 in the structure of Cu(I)-AZAMI-F (loop sequence CTPHPM) at pH 6,[25] which has a higher pK_a (5.9) for His115, although the ligand-containing loop is one residue shorter. This hydrogen bond could contribute to the elevated pK_a values in the AZ loop mutants. However, the same hydrogen bond could also form in WT AZ if the His117 ligand protonated and rotated.[27] Furthermore, in the structure of WT Cu(I)-AMI in which His95 is protonated and the imidazole is rotated,[7] the N$^{\varepsilon 2}$ atom is 4.3 Å from the backbone carbonyl oxygen of Pro52, and therefore this hydrogen bond is absent. A clear relationship between hydrogen bonding and the pK_a of the histidine ligand is difficult to discern.

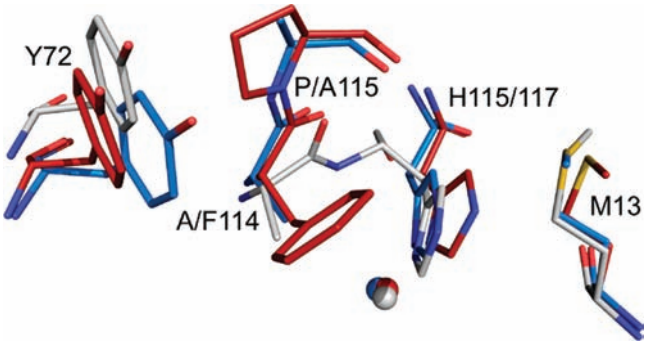

Figure 5. A comparison of the interactions involving the histidine ligand on the ligand-containing loop in Cu(I)-AZ at pH 5.5 (dark red), Cu(I)-AZ2A2A at pH 7 (gray), and Cu(I)-AZ4A4A at pH 7 (blue). These interactions are very similar in AZ4A3A[30] as in AZ4A4A, and therefore the structure of AZ4A3A is not included.

The Influence of Other Second Coordination Sphere Features on the Histidine Ligand pK_a. Other second coordination sphere interactions, particularly those involving the imidazole of the histidine ligand, can also tune the pK_a of this residue.[18,20,26] For example, recent studies on PAZ and PC have shown that π-interactions with the imidazole of the histidine ligand influence the pK_a value by ∼1 pH unit.[26] In AZ, His117 is sandwiched between Phe114 and Met13 (Figure 5).[39] The environment of the histidine ligand is influenced by mutations to the C-terminal loop, and the use of only alanine residues in this region can have a particularly large effect. In AZ2A2A, AZ4A3A, and AZ4A4A, Phe114 is absent (the C$^{\beta}$ of Ala114 is in a very similar position as the C$^{\beta}$ of Phe114), with the replacement of the phenyl ring by a methyl moiety resulting in movement of the side chain of Tyr72 (Figure 5) and an increased number of solvent molecules in this location. The side-chain orientation of Met13 is altered in the polyalanine loop variants, but the interaction with the histidine ligand is not dramatically affected. The contacts of His117 with Phe114 and Met13 have been suggested as a contributing factor to the low pK_a of His117 in

(45) Barrett, M. L.; Harvey, I.; Sundararajan, M.; Surendran, R.; Hall, J. F.; Ellis, M. J.; Hough, M. A.; Strange, R. W.; Hillier, I. H.; Hasnain, S. S. *Biochemistry* **2006**, *45*, 2927–2939.
(46) Guss, J. M.; Freeman, H. C. *J. Mol. Biol.* **1983**, *169*, 521–563.
(47) Cunane, L. M.; Chen, Z.; Durley, R. C. E.; Mathews, F. S. *Acta Crystallogr.* **1996**, *D52*, 676–686.
(48) Inoue, T.; Nishio, N.; Suzuki, S.; Kataoka, K.; Kohzuma, T.; Kai, Y. *J. Biol. Chem.* **1999**, *274*, 17845–17852.
(49) Velarde, M.; Huber, R.; Yanagisawa, S.; Dennison, C.; Messerschmidt, A. *Biochemistry* **2007**, *46*, 9981–9991.

AZ.[50] These interactions in AZ result in His117 being buried from solvent, which has also been highlighted as a determinant of the pK_a for the histidine ligand in cupredoxins.[9,27] The C-terminal histidine ligand is more exposed in AZ2A2A and AZAMI (solvent accessibilities of 32 and 21 Å^2, respectively) than in AZ4A3A, AZ4A4A, and AZ where it seems to be equally protected (5−8 Å^2 accessible to solvent). The solvent accessibility of the histidine ligand alone therefore cannot account for the effects that we observe in the polyalanine loop mutants.

Conclusions

Structural features that influence the pK_a of the C-terminal histidine ligand at a T1 copper site have proven difficult to identify. In this study, we show that the length of a ligand-containing polyalanine loop does influence the pK_a of this coordinating residue. The influence of loop length that we observe could be due to a number of factors because even with the use of relatively simple polyalanine loops, alterations in length influence other active site properties, which can affect the pK_a value, particularly the solvent exposure of the histidine ligand. The hydrogen-bonding pattern at the active site seems to have a limited effect on the pK_a of the histidine ligand. Shortening the ligand-containing loop could decrease flexibility in this region and possibly introduce strain, facilitating histidine ligand protonation. The use of only alanine residues in the loop results in the influence of loop length on the pK_a value of the histidine ligand being diminished compared with native loop sequences. Many of the residues in the loop contribute to the second coordination sphere, and therefore length and sequence have a major influence on this aspect of the active site. A longer loop increases the possible number of second coordination sphere interactions, which, along with the length of the loop, can prevent protonation of the histidine ligand in the accessible pH range. A shorter loop, particularly between the cysteine and histidine ligands, decreases the second coordination sphere and limits the possibilities for tuning the pK_a value.

Acknowledgment. This work was supported by Biotechnology and Biological Sciences Research Council Grant BB/C504519/1 (to C.D.). M.J.B. is supported by a Royal Society (United Kingdom) University Research Fellowship.

(50) Canters, G. W.; Kalverda, A. P.; Hoitink, C. W. G. In *The Chemistry of the Copper and Zinc Triads*; Welch, A. J., Chapman, S. K., Eds.; The Royal Society of Chemistry: Cambridge, 1993; pp 30−37.